Relative predictive value of lung cancer screening CT versus myocardial perfusion attenuation correction CT in the evaluation of coronary calcium

Grant Bailey[1,2], **Abigail Healy**[1,3,4], **Bryan D. Young**[1,2], **Esseim Sharma**[3,4], **Judith Meadows**[1,2], **Hyung J. Chun**[2], **Wen-Chih Wu**[3,4], **Gaurav Choudhary**[3,4], **Alan R. Morrison**[1,2,3,4] *

1 Department of Internal Medicine (Section of Cardiovascular Medicine), VA Connecticut Healthcare System, West Haven, Connecticut, United States of America, **2** Department of Internal Medicine (Section of Cardiovascular Medicine), Yale Cardiovascular Research Center, Yale University School of Medicine, New Haven, Connecticut, United States of America, **3** Department of Internal Medicine (Section of Cardiovascular Medicine), Providence VA Medical Center, Providence, Rhode Island, United States of America, **4** Department of Internal Medicine (Section of Cardiovascular Medicine), Alpert Medical School of Brown University, Providence, Rhode Island, United States of America

* alan_morrison@.brown.edu

Abstract

Coronary artery calcium scores (CACS) from lung cancer screening computed tomography (LCSCT) or myocardial perfusion attenuation correction computed tomography (ACCT) are not routinely performed or reported. CACS from LCSCT and ACCT have not been directly compared in the same patient population. We identified 66 patients who underwent both LCSCT (non-gated) and ECG-gated cardiac CT (CCT) within a 2-year span. Of this population, 40 subjects had also undergone ACCT. Using the Agatston method, CACS for 264 individual vessels from the LCSCT population and for 160 vessels from ACCT population were calculated and evaluated for agreement with ECG-gated CCT as the gold standard. Secondary analysis included a comparison of individual vessel contribution to variations in agreement and a comparison of total CACS from CCT, LCSCT, and ACCT for respective MACE prediction. CACS from LCSCT demonstrated a strong Pearson correlation, $r = 0.9017$ (0.876–0.9223), with good agreement when compared to CACS from CCT. CACS from ACCT demonstrated a significantly (P < 0.00001) weaker correlation, $r = 0.5593$ (0.4401–0.6592). On an individual vessel basis, CACS from all major vessels (LM, LAD, LCX, and RCA) contributed to the weaker correlation. For total vessel CACS, LCSCT demonstrated comparable area under the curve (AUC) for the receiver operating characteristic (ROC) curve (LCSCT AUC = 0.8133 and CCT AUC = 0.8302, P = 0.691) for prediction of MACE. Although ACCT demonstrated a similar AUC (ACCT AUC = 0.7969, P = 0.662) for MACE prediction the cutoff value for elevated risk was extremely low. In conclusion, LCSCT outperformed ACCT at calcium scoring by providing better agreement and comparable risk assessment to CCT despite the absence of ECG-gating. It is therefore reasonable to use LCSCT images to derive and report Agatston-based CACS for cardiovascular risk

Abbreviations: ACCT, Attenuation correction computed tomography; ASCVD, Atherosclerotic cardiovascular disease; AUC, Area under the curve; BMI, Body mass index; CABG, Coronary artery bypass graft surgery; CACS, Coronary artery calcium score; CAD, Coronary artery disease; CCT, ECG-gated cardiac computed tomography; CT, Computed tomography; DM, Diabetes mellitus; ECG, Electrocardiography; HU, Hounsfield Units; keV, Kiloelectron volts; LAD, Left anterior descending; LCSCT, Lung cancer screening computed tomography; LCx, Left circumflex; LM, Left main; MACE, Major adverse cardiac events; mAmp, Milliamperes; MI, Myocardial infarction; PACS, Picture archiving communication system; PCI, Percutaneous intervention; PET, Positron emission tomography; RCA, Right coronary artery; ROC, Receiver operating characteristic; SEE, Standard error of the estimate; SPECT, Single-photon emission computed tomography; VA, Veterans Affairs.

assessment, whereas the use of ACCT images to report Agatston-based CACS is not currently practical.

Introduction

According to the World Health Organization, ischemic heart disease caused by atherosclerotic coronary artery disease (CAD) remains the single leading cause of morbidity and mortality in the world[1]. Calcification of atherosclerotic plaques is a well-established pathologic finding that carries predictive value in terms of atherosclerotic burden and risk of cardiovascular mortality and all-cause mortality[2, 3]. In addition, the organization of calcific deposits within individual atherosclerotic plaque has predictive value for the plaque's vulnerability[4–6]. ECG-gated CCT defines coronary calcium by a threshold attenuation coefficient measurement of 130 Hounsfield units (HU) with an area of ≥ 1 mm^2, and CACS are then determined by the product of calcified plaque area and relative density as determined by attenuation[7]. Other large epidemiologic studies have used a threshold of 130 HU with an area of ≥ 1.48 mm^2 to identify coronary calcium[8, 9]. In line with the goals of precision medicine, the addition of coronary artery calcium score to prediction models based on traditional risk factors significantly improves risk stratification and can place more individuals in the most extreme risk categories, thus having potential to influence decision making with regards to medical therapy [10, 11].

Lung cancer, the third most common cancer and leading cause of cancer-related death, can be treated with surgical resection which is potentially curative in early stages[12, 13]. Low-dose, non-gated, noncontrast chest CT (LCSCT) scans have provided a significant benefit for lung cancer screening in the high-risk smoking population and are recommended for routine cancer screening[13–17]. Because smoking is also a major risk factor for ischemic heart disease and there is significant overlap between eligibility for LCSCT and elevated cardiovascular risk, there is broad interest in using information about coronary calcification from LCSCT to aide in cardiovascular event risk assessment[18–21]. In the evaluation of myocardial ischemia, hybrid imaging using either single-photon emission computed tomography (SPECT) or positron emission tomography (PET) combined with CT allows for improved diagnostic accuracy of myocardial perfusion imaging through the use of CT-based attenuation correction algorithms[22–26]. Moreover, there may be additional benefit to assessing coronary calcium on attenuation CT scans during myocardial perfusion imaging to help further predict cardiovascular event risk[27–29].

While studies have demonstrated reasonable agreement between CACS from various types of non-gated, noncontrast chest CT and ECG-gated CCT, clinical outcomes have rarely been evaluated[30–34]. Conversely, recent studies that demonstrated the predictive value of CACS from LCSCT did not directly compare LCSCT with the gold standard, ECG-gated CCT, for agreement[19, 20]. Moreover, despite showing strong potential for providing information about coronary artery calcium burden, there has been no direct comparison of ACCT with CCT in terms of Agatston CACS values or MACE prediction[27–29]. Lastly, there have been no studies that directly compare both LCSCT and ACCT with CCT in the same population.

Here, we identified a patient population who had undergone LCSCT, ACCT, and CCT within a 2-year period. We evaluated agreement and predictive value of Agatston-based CACS from LCSCT and ACCT scans compared to CCT as a gold standard. To our knowledge, this is

the first direct evaluation of both LCSCT and ACCT relative to CCT for the prediction of outcomes in an elevated risk population, using a standard Agatston-based scoring method.

Materials and methods

This study was approved by the VA Connecticut Healthcare Institutional Review Board and complies with the Declaration of Helsinki, and all patient data were handled in compliance with the Health Insurance Portability and Accountability Act (HIPAA) regulations. All patient records were de-identified and analyzed anonymously.

Study design and patient population

We undertook a retrospective study design. This study was performed at a single site, the Veterans Affairs (VA) Healthcare System Medical Center in West Haven, Connecticut. This study included all U.S. Veterans who were identified as having undergone both LCSCT and CCT within a 2-year period between October 1, 2012 and September 30, 2015. We identified 66 patients that met these criteria. Of the 66 patients, 40 patients had also undergone a myocardial perfusion imaging study with ACCT within the same 2-year period.

CT acquisition and reconstruction parameters

Table 1 summarizes all CT Acquisition and Image Reconstruction Parameters.

1. CCT.   Studies at the West Haven VA Medical Center were performed using a 64-slice CT scanner (Toshiba Acquilion) with a 64 mm x 0.5 mm collimation, using an axial acquisition protocol. Rotation time was 0.23 seconds. All scans were ECG-gated and electrocardiographically triggered at 70% of the R-R interval, with patient heart rates averaging between 55–65 BPM. Scanning field of view was set to 320 mm. Matrix size was 256 x 256. Based on these parameters, the minimum area required to identify calcium was 1.56 mm^2. A 120-kV tube voltage was applied for all subjects. The tube current was 73 mAmp. Image reconstruction slice thickness was 3 mm.

2. LCSCT.   Studies at the West Haven VA Medical Center were performed using a 64-slice CT scanner (Toshiba Acquilion) with a 64 mm x 0.5 mm collimation, using a helical acquisition protocol. Rotation time was 0.35–0.4 seconds, and pitch was 0.84. Studies were not ECG-gated, and patient heart rates were not controlled. Scanning field of view was set to 400 mm. Matrix size was 256 x 256. Based on these parameters, the minimum area required to identify calcium was 2.44 mm^2. The average tube voltage was 100 kV, and the tube current was modulated between 50–70 mAmp. Image reconstruction slice thickness was 2 mm.

3. ACCT.   Studies at the West Haven VA Medical Center were performed using a 16-slice CT scanner (Phillips Precedence) with a 16 mm x 1.5 mm collimation, using a helical acquisition protocol. Rotation time was 0.4 seconds, and pitch was 0.81. Studies were not ECG-gated, and patient heart rates were not controlled. Scanning field of view was set to 600 mm. Matrix size was 512 x 512. Based on these parameters, the minimum area required to identify calcium was 1.37 mm^2. A 120-kV tube voltage was applied for all subjects. The tube current was 30 mAmp. Image reconstruction slice thickness was 5 mm.

Coronary artery calcium scoring

For CCT, LCSCT, and ACCT scans, CACS was calculated using the Agatston method[7]. Coronary artery calcium scoring was performed using previously described methods for other epidemiologic studies[8, 9], and images were viewed and scored using a Carestream Vue PACS (Carestream Health) imaging workstation. In brief, the calcium scoring application in the

Table 1. CT acquisition and image reconstruction parameters.

	CCT	LCSCT	ACCT
Collimation	64 x 0.5 mm	64 x 0.5 mm	16 x 1.5 mm
Acquisition Protocol	Axial	Helical	Helical
Rotation Time	0.23	0.35–0.4	0.4
Pitch	N/A	0.84	0.81
FOV	320	400	600
Matrix Size	256 x 256	256 x 256	512 x 512
Area Required to Identify Calcium	≥ 1.56 mm^2	≥ 2.44 mm^2	≥ 1.37 mm^2
Tube Voltage	120 kVp	100 kVp	120 kVp
Tube Current	73 mAmp	50–70 mAmp	30 mAmp
Image Reconstruction Slice Thickness	3.0 mm	2.0 mm	5.0 mm
Average Slices Containing the Heart, mean ± s.d. (P value)	32 ± 5.5 (<0.0001)	44 ± 5.1 (<0.0001)	22 ± 4.9 (<0.0001)

P value relative to other CT values, as determined by ordinary one-way ANOVA followed by Tukey's post hoc multiple comparisons test.

https://doi.org/10.1371/journal.pone.0175678.t001

Carestream Vue PACS displays axial image slices for the reader. The calcium scoring application was equally successful at presenting axial images from CCT, LCSCT, and ACCT. As expected, the mean numbers of slices taken up by the heart on axial images were statistically different 32 ± 5.5, 44 ± 5.1, and 22 ± 4.9 for CCT, LCSCT, and ACCT studies, respectively (see Table 1). The reader scrolls through axial slices and identifies coronary arteries with potential calcium to be scored. The reader indicates the appropriate coronary vessel to the program and circles the region of interest. Only pixels of attenuation coefficient measurements above 130 HU within the region of interest are selected as calcified and incorporated into the calcium score. All scans were scored twice; once by a board-certified cardiologist in Cardiovascular Computed Tomography (A.R.M. and J.M) and once by a cardiac imaging residents and fellows (G.B., E.S., and B.D.Y.). Residents and fellows were trained on 50 scans with feedback and supervision from the board-certified cardiologists. All readers were blinded to patient clinical data and the calcium scores from the different CT modalities (CCT, LCSCT, and ACCT). Inter-observer agreement was quantified for total CACS values from all (CCT, LCSCT, and ACCT) studies, and the overall kappa was found to be very good at 0.915 with 95% confidence interval from 0.867 to 0.964.

Covariates

The electronic medical record was searched for patient demographics and cardiovascular covariates including age, sex, race, and BMI. Medical history included smoking status, hypertension, hypertensive medication, cholesterol medication, diabetes and diabetes medication, and fasting lipid profile. 10-Year Framingham risk score and ASCVD risk score were calculated.

Outcomes

The electronic medical record was searched for major adverse cardiovascular events (MACE) as defined by death by all cause, sudden cardiovascular death, death by cerebrovascular accident, nonfatal cerebrovascular accident, nonfatal myocardial infarction, acute coronary syndrome, and revascularization by either percutaneous intervention (PCI) or coronary artery bypass graft surgery (CABG).

Statistical analysis

All statistical data were analyzed with the use of Prism 6 (GraphPad) or R software version 3.3.1 (R Core Team). Baseline demographics, clinical characteristics, and CACS were compared between the cohort that underwent LCSCT and the subgroup who also underwent ACCT. Results are presented as mean (standard error) for continuous variables with normal distribution, as median (interquartile range) for continuous variables without normal distribution, and as number (percentage) for categorical data. The t test was used to compare normally distributed continuous variables between 2 independent groups. The Wilcoxon rank sum test was used for continuous variables not normally distributed, and Chi-square test was used for categorical variables. Differences between multiple groups were assessed by ANOVA followed by Tukey's post hoc multiple comparisons test. For analysis of CACS between LCSCT and CCT or ACCT and CCT, the Pearson product-moment correlation coefficient was determined followed by a Bland-Altman plot for bias and agreement. Analyses were repeated using Generalized Estimating Equations (GEE) to adjust for potential clustering of coronary vessel's calcium score by patient. For receiver operating characteristic curves, comparison of the areas under the curve between LCSCT and CCT as well as between ACCT and CCT were carried out by the method established by Hanley and McNeil[35]. Time-to-event curves using the Kaplan-Meier method were calculated. Results were compared using the log-rank statistic. A 2-sided $P < 0.05$ was considered statistically significant. Using a two-sided alpha of 0.05, our study had an 80% power to detect a 10% difference in the Pearson correlation between LCSCT and ACCT. Using a two-sided alpha of 0.05, our study had an 80% power to detect significance in the proportion of events using calcium score cutoff for CCT.

Results

We evaluated a total of 66 patients who had undergone both LCSCT and CCT within the period of 3 years between October 1, 2012 and September 30, 2015 (Table 2). The 66 patients in this study had a mean age of 65 years. All patients were U.S. Veterans. A majority of the patients were white men and smokers with elevated cardiovascular risk. The median cholesterol was 169 mg/dL and the median BMI was 31 kg/m^2. Approximately one-third of the patients carried a history of diabetes or a family history of early CAD. Fifteen percent of patients had known CAD by a prior imaging modality, but none of the patients had a previous history of revascularization. Of the 66 patients, 40 patients had also undergone myocardial perfusion imaging with ACCT. There were no differences in the demographics and clinical characteristics between the patients who underwent LCSCT and the patients who underwent both LCSCT and ACCT (Table 2). The median CACS as determined by CCT from both LCSCT and the ACCT populations was comparable at 160 and 176 (P = 0.731), respectively. The median time between CCT and non-gated CT was 7 (IQR: 1,17) months for LCSCT and 2 (IQR: 1,5) months for ACCT.

The agreement of individual coronary artery CACS between either LCSCT (264 coronary arteries) or ACCT (160 coronary arteries) and CCT were evaluated (Fig 1). Despite the lack of ECG-gating, the Pearson correlation between CACS from the CCT and the CACS from LCSCT was strong at 0.9017 (SEE = 6.4, P < 0.0001). Bland-Altman analysis showed a mean bias of -2 with 95% limits of agreement between -130 to 127. The Pearson correlation between CACS from the CCT and the CACS from ACCT was 0.5593 (SEE = 58.5, P < 0.0001). The Bland-Altman analysis showed a mean bias of -61.7 with 95% limits of agreement between -293 to 169. The Pearson correlations were statistically different between the LCSCT and the ACCT CACS (P < 0.00001). Results did not significantly change after adjusting for potential clustering effect at the individual patient level.

Table 2. Baseline demographics, clinical characteristics, and CACS of LCSCT vs. ACCT populations.

	LCSCT (*n* = 66)	ACCT (*n* = 40)	P Value
Age, years, median (IQR)	65 (58, 67)	65 (59, 67)	0.919
BMI, median (IQR)	31 (26, 35)	31 (27, 34)	0.987
Male, *n* (%)	61 (92)	37 (93)	0.715
Caucasian, *n* (%)	57 (86)	34 (85)	0.927
African American, *n* (%)	9 (14)	6 (15)	0.927
DM, *n* (%)	19 (29)	12 (30)	0.931
Hypertension, *n* (%)	49 (74)	29 (73)	0.976
Hyperlipidemia, *n* (%)	43 (65)	31 (78)	0.261
Total Cholesterol, median (IQR)	169 (145, 201)	171 (147, 204)	0.825
HDL Cholesterol, median (IQR)	36 (36, 55)	41 (36, 54)	0.759
Statin Use, *n* (%)	39 (59)	29 (73)	0.235
Smoking, *n* (%)	51 (77)	29 (73)	0.748
Family History of Early CAD, *n* (%)	20 (30)	16 (40)	0.487
CAD, *n* (%)	10 (15)	9 (23)	0.487
MI, *n* (%)	1 (2)	1 (3)	0.708
Prior PCI or CABG, *n* (%)	0 (0)	0(0)	N/A
Framingham Risk, median (IQR)	16 (12, 19)	16 (13, 18)	0.809
ASCVD Risk, median (IQR)	22 (15, 28)	21 (16, 28)	0.868
CCT CACS, median (IQR)	160 (14, 441)	176 (18, 500)	0.731

BMI = body mass index; DM = diabetes mellitus; CAD = coronary artery disease; MI = myocardial infarction; PCI = percutaneous intervention; CABG = coronary artery bypass graft surgery; ASCVD = atherosclerotic cardiovascular disease; CT = computed tomography; CACS = coronary artery calcium score; AC = attenuation correction

We assessed whether any individual vessel calcium scores contributed more or less to the significantly decreased agreement of ACCT-derived CACS (Table 3). The CACS were divided by individual vessel and then each vessel CACS was compared for agreement with the respective CACS from CCT studies as the gold standard. The Pearson correlations for the LCSCT studies were 0.9599 (0.9349–0.9754), 0.929 (0.8854–0.9564), 0.9169 (0.8668–0.9486), and 0.8548 (0.7702–0.9099) for left main (LM), left anterior descending (LAD), left circumflex (LCX), and right (RCA) coronary arteries, respectively. The Pearson correlations for the ACCT studies were 0.8424 (0.7176–0.9148), 0.5134 (0.2272–0.718), 0.7246 (0.5304–0.8466), and 0.5393 (0.2696–0.7305) for LM, LAD, LCX, and RCA respectively. On an individual vessel basis, the ACCT demonstrated decreased agreement relative to LSCST for all four major vessels, indicating that the weaker correlation is global and not particular to any specific vessel, nor attributable to the lack of ECG-gating or motion artifact of any one vessel. Fig 2 demonstrates an example of the discrepancy in agreement between images from ACCT and images from both LCSCT and CCT with areas of visually appreciable calcium in the LAD that fell below the Agatston threshold of 130 HU on the ACCT image (ACCT, upper panel, yellow arrow), leading to an under-identification of the calcium burden in the ACCT study.

In our patient population, the median follow-up time for MACE was 24 (IQR: 20, 24) months for LCSCT and CCT, and 24 (IQR: 16, 24) months for ACCT, and there was a total of 12 MACE events; 1 cardiac death, 2 noncardiac deaths, 1 CVA, 2 CABGs and 6 PCIs. Fig 3 demonstrates the receiver operating characteristic (ROC) curves for the three imaging modalities of CCT, LCSCT and ACCT. The AUC for the ROC curves were 0.8302 (95% confidence interval: 0.7112 to 0.9493), 0.8133 (95% confidence interval: 0.6922 to 0.9344), and 0.7969
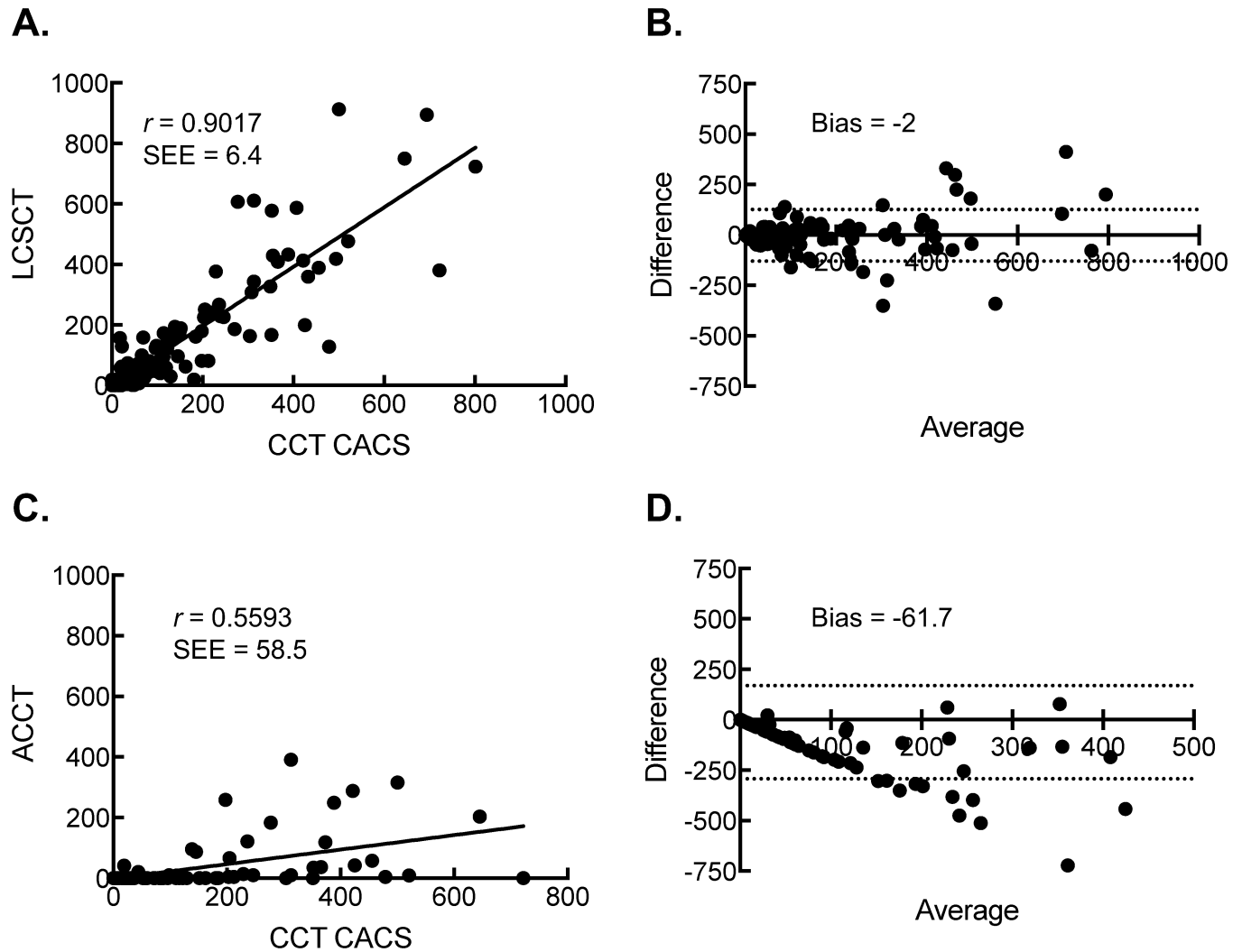
Fig 1. Scatter plot of Agatston CACS from CCT scans and either LCSCT or ACCT scans along with corresponding Bland-Altman plots for agreement. (A) The Pearson correlation of CACS between CCT scans and LCSCT scans. (B) Bland-Altman Plots for Agreement between CCT scans and LCSCT scans. (C) The Pearson correlation of global CACS between CCT scans and ACCT scans. (D) Bland-Altman Plots for Agreement between CCT scans and ACCT scans.

(95% confidence interval: 0.624 to 0.9698) for CCT, LCSCT, and ACCT, respectively. Comparison of the AUCs revealed no significant differences between LCSCT and CCT (P = 0.691), ACCT and CCT (P = 0.678), or LCSCT and ACCT (P = 0.839). Despite comparable sensitivity and specificity among the three tests, the cutoff values for optimal test performance were quite different. At CACS of >250, the CCT scans had an 83% sensitivity and a 72% specificity with a likelihood ratio of 3 for MACE in this patient population. Comparable performance could be obtained at CACS >200 and CACS >10 for LCSCT and ACCT, respectively.

Based on the AUC derived from the ROC curves, patients were divided into high and low risk groups, using the above cutoff values for optimal test performance. Fig 4 demonstrates the Kaplan-Meier plots for MACE outcomes (CACS high-risk cutoffs of >250 for CCT, >200 for LCSCT, and >10 for ACCT). The plots for the low-risk vs. high-risk groups were statistically significant in all CT modalities. When the low risk plots were compared between CCT, LCSCT, and ACCT, there were no statistical differences (P = 0.8818) between the CT

Table 3. Comparison of the Pearson correlation of total CACS and individual vessel CACS between LCSCT and ACCT.

Vessel	LCSCT r (95% CI)	ACCT r (95% CI)	P Value
Total	0.9385 (0.9007–0.9621)	0.6204 (0.3751–0.7845)	< 0.00001
LM	0.9599 (0.9349–0.9754)	0.8424 (0.7176–0.9148)	0.0006
LAD	0.929 (0.8854–0.9564)	0.5134 (0.2272–0.718)	< 0.00001
LCX	0.9169 (0.8668–0.9486)	0.7246 (0.5304–0.8466)	0.0016
RCA	0.8548 (0.7702–0.9099)	0.5393 (0.2696–0.7305)	0.0012

https://doi.org/10.1371/journal.pone.0175678.t003

modalities. Likewise, when the high-risk plots were compared between CCT, LCSCT, and ACCT, there were no differences (P = 0.784) between the CT modalities.

Discussion

We evaluated the significance of Agatston-derived CACS values derived from LCSCT and ACCT scans in an elevated risk population and found that LCSCT demonstrated better
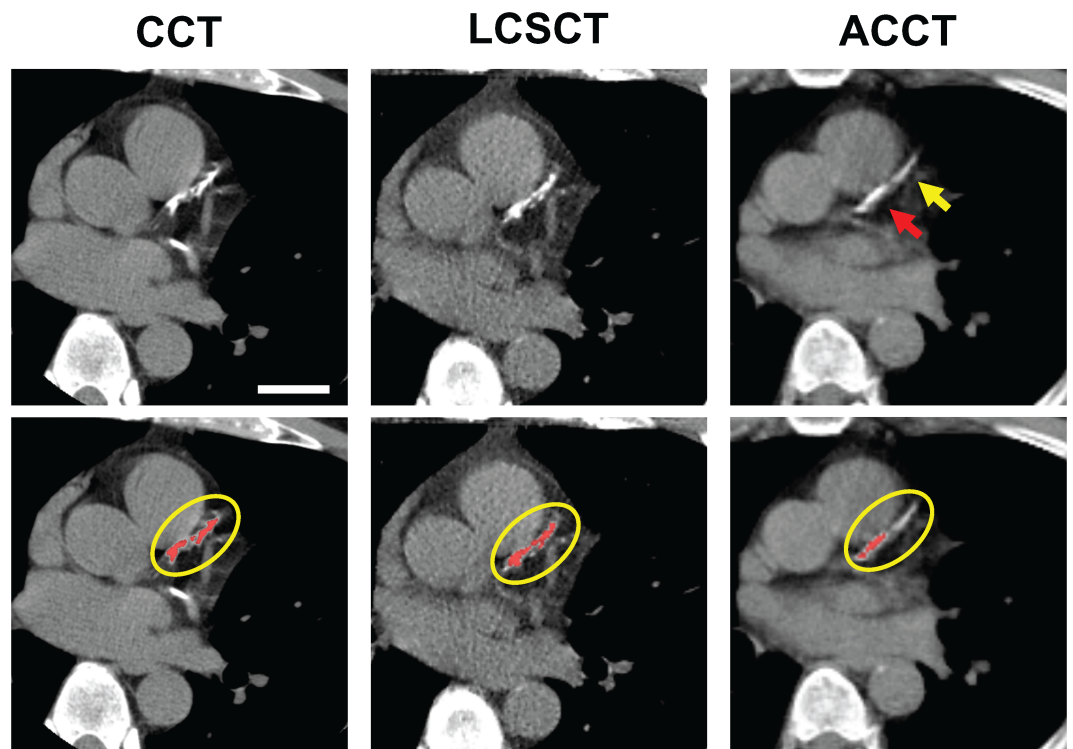

Fig 2. Example of the decreased detection of calcium using ACCT relative to CCT and LCSCT in a single slice plane of the LAD from an individual patient. CCT with LAD Agatston CACS of 645. LCSCT with LAD Agatston CACS of 749. ACCT with LAD Agatston CACS of 203. Bar, 3cm. Upper panel; CT images at the level of the proximal to mid LAD. Red arrow; identified calcium. Yellow arrow; unidentified calcium. Lower panels; CT images as displayed at the imaging workstation with pixels of Agatston threshold of 130 Hounsfield units (HU) highlighted in red and region of interest circled in yellow. In this example, LCSCT images were acquired 14 months after the CCT images and the ACCT images were acquired 3 months prior to the CCT images.
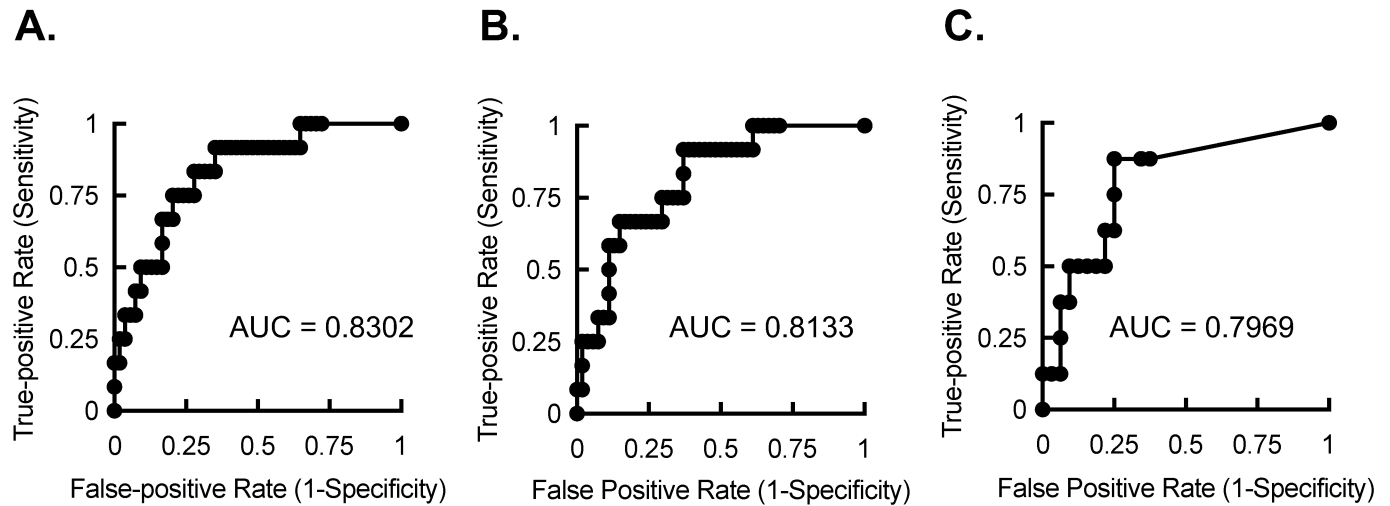
https://doi.org/10.1371/journal.pone.0175678.g002

A.

B.

C.

Fig 3. Receiver operator characteristic curves for CCT, LCSCT, and ACCT. (A) ROC curve for CCT with AUC of 0.8302 (P = 0.0004). (B) ROC curve for LCSCT with AUC of 0.8133 (P = 0.0007). (C) ROC curve for ACCT with AUC of 0.7969 (P = 0.01).

https://doi.org/10.1371/journal.pone.0175678.g003

agreement with ECG-gated CCT as the gold standard. Secondary analysis confirmed that no individual vessel was responsible for the lower agreement by ACCT. Though LCSCT and ACCT demonstrated comparable area under the curve (AUC) for the receiver operating characteristic (ROC) curve, cutoff values for elevated risk and optimal test performance revealed LCSCT performs in a manner comparable to CCT. There is robust data to support the use of coronary artery calcium scoring in the further risk stratification of patients with elevated cardiovascular risk[36]. Moreover, a calcium score of zero carried a negative predictive value of 96% for stenosis greater than 50% in a large study of symptomatic patients[37]. However, coronary calcium scoring for precision cardiovascular risk stratification of patients remains underutilized. Furthermore, most insurance providers do not cover the expense of a standard CCT for CACS, and some even consider CCT for CACS to be investigational[31, 36]. In addition to cost, concerns have been raised by studies that have projected a small and finite increase in lifetime cancer risk attributable to CCT, despite technological advances and guidelines that have reduced the radiation exposure below 1 mSv[38, 39]. Thus, demonstrating ability to obtain comparable data regarding coronary calcification from alternative methods may fulfill a large, unmet clinical need. There are an estimated 72 million noncontrast chest CTs done each year in the U.S.[40]. With the recent U.S. Preventative Services Task Force recommendations for lung cancer screening with low-dose computed tomography in adults who have a long-standing history of smoking, the use of LCSCT is expected to grow tremendously; it is estimated that as many as 94 million U.S. adults are current or former smokers[15, 41]. Our current study assessed the utility of reporting CACS from these studies to provide cardiovascular risk assessment and clinical management benefit with negligible added expense or radiation exposure.

We identified CACS values from LCSCT studies as essentially comparable to those from CCT despite the lack of ECG-gating. Recently, LCSCT was determined to underestimate calcium score, particularly in the lower range (<1000) of calcium scores[31]. There are several technical explanations for our study's improved agreement in the lower range calcium scores. First, by performing our analysis on individual vessel CACS values, we were able to increase the power of our study while focusing on CACS values <800. Second, our study was unique in
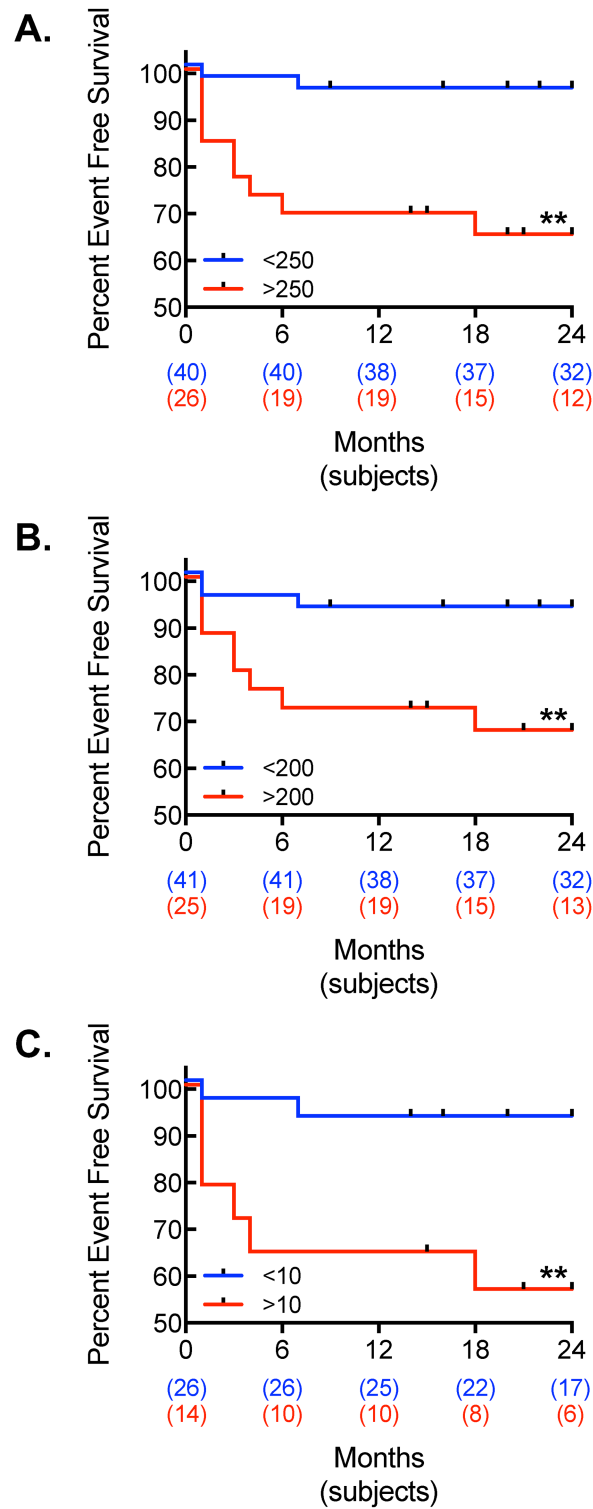
Fig 4. Kaplan-Meier plots for MACE. Kaplan-Meier event curve for MACE using (A) CCT, (B) LCSCT, and (C) ACCT in patients divided into low and high calcium burden as determined by their respective ROC Curves (**, P < 0.01, log-rank test).

https://doi.org/10.1371/journal.pone.0175678.g004

that we used dedicated lung cancer screening CT scans that had image reconstruction slice thicknesses of 2 mm, which is a comparable thickness to the standard of 2.5 mm ECG-gated cardiac CT scans. The prior study used CACS derived from whole body CT scans with image reconstruction thickness of 6 mm and included a large proportion of CACS values in excess of 1000[31]. Finally, the prior study used CT studies that were performed on an older model electron beam CT scanner between 2000 and 2003, while our study used CT images acquired on a newer 64-slice thickness CT scanner between 2012 and 2015.

Recently, CACS derived from ACCT have demonstrated good agreement, using subjective estimations of calcium burden based on a visual scoring system[27]. Our study differed in that we took a standardized approach to acquisition and scoring that eliminated subjectivity, potential variability among less experienced users, and the increased risk of false positive identification of calcium. By using a more universally applicable and standardized approach, we identified a significantly weaker agreement with a strong negative bias in calcium scores from ACCT studies. Recent studies have sought to change scan acquisition or the thresholding for calcification to <130 HU to make up for the reduced detection of calcium on ACCT scans[28, 29]. Fig 2 illustrates an example of visually appreciable calcium in the LAD that was under-identified because it did not meet the 130 HU threshold for calcium scoring. However, it remains unclear whether reducing the threshold would reduce or sacrifice the specificity of calcium detection, and thus further study is needed in this area.

Coronary artery motion, particularly the motion of the right coronary artery (RCA), during cardiac phases is highly susceptible to imaging artifact in the absence of ECG-gating[42]. However, ECG-gating did not appear to affect the identification of calcium by LCSCT, and results from the individual vessel analysis demonstrated that all four vessels rather than just the RCA contributed to the under identification of calcium on the ACCT studies. Moreover, rotation time and pitch were comparable between LCSCT and ACCT acquisition protocols, indicating that they are not likely to be contributing to the differences in calcium detection. Several alternative explanations for the decreased identification of calcium on ACCT studies remain to be studied. Foremost, the ACCT images were reconstructed at the standard 5 mm slice thickness, whereas the CCT and LCSCT images were reconstructed at 2.5 and 2 mm, respectively. Consistent with the increased slice thickness is the reduced number of slices containing the heart on the ACCT axial images; thus, the under-identification of calcium associated with ACCT may have been influenced by partial volume effects, leading to reduced attenuation measures. Drawing absolute conclusions about image reconstruction thickness from the data is confounded by the other differences in scanning and reconstruction parameters, including collimation, matrix size, and field of view (Table 1). However, field of view and matrix size contribute the minimal pixel area required to identify calcium, and thus it is interesting to note that LCSCT had the largest minimal calcium area of 2.4 mm^2 whereas ACCT had the smallest minimal area at 1.37 mm^2, suggesting that these parameters were less likely to contribute to an under-identification of calcium in ACCT studies. Future studies that compare variation in calcium identification conferred by image reconstruction thickness while holding these other acquisition and reconstruction parameters constant are required to understand the extent to which reconstruction thickness impacts calcium score. In addition, we cannot rule out other technical differences from the ACCT scanner, particularly the intrinsic wider collimation, which may also theoretically cause partial volume effects that decrease sensitivity for detection of calcium. Further research is clearly needed to delineate the respective influences of image reconstruction thickness, acquisition parameters of collimation, matrix, and field of view, and scanner type.

We also identified that CACS from LCSCT and CCT had essentially equivalent predictive power for outcomes. This was consistent with other studies evaluating low-dose, noncontrast

CT scans in asymptomatic populations[19, 31], however, our study differed in that it was a direct comparison of dedicated LCSCT with CCT in an elevated risk population using comparable image reconstruction thickness. The ROC curves for ACCT and CCT were similar though, as expected, the absolute CACS cutoff values for comparable sensitivity and specificity differed between the imaging approaches. It is possible that our study is underpowered to detect a significant difference in the AUCs between ACCT and CCT, but from a practical perspective there is likely little clinical meaning in the difference between AUCS of 0.8302 and 0.7969. However, the major difference is in the utility of the significantly lowered threshold of optimal test performance for indicating elevated event risk in the ACCT study. Whereas similar risk assessment standards established by CCT can be applied to LCSCT because of the similar test performance and similar absolute CACS values, such standards could not be applied to ACCT without marked reductions in sensitivity and negative predictive value.

There are a number of limitations to this study that must be acknowledged. This was a retrospective study design that took place at a single institution. Our sample size was relatively small and events were primarily driven by revascularization, and so it will be important to confirm these findings in a larger, prospective study designed to include cardiovascular events. Finally, further studies regarding image reconstruction thickness and scanner limitations are required before any final conclusions can be drawn about the potential utility of ACCT derived CACS.

Conclusions

In summary, CACS by the Agatston method can be readily carried out in LCSCT and ACCT studies. Despite a lack of ECG-gating, the CACS from LCSCT can be considered as essentially comparable to CACs from ECG-gated CCT in terms of absolute value and predictive power, provided image reconstruction thickness and scanner type are similar as they were in this study. CACS from ACCT tended to under-identify coronary calcification. Though ACCT retained a similar AUC for the ROC curve relative to CCT, the cutoff for optimal test performance was markedly lower such that it would be difficult to practically assess CACS in ACCT studies. Thus, it is currently not reasonable to use Agatston-derived CACS values from ACCT images; however, more studies will be required to ultimately define whether alternative assessments of coronary calcification using ACCT can aid in the assessment of cardiovascular risk. Nevertheless, standard reporting of Agatston CACS from LCSCT is accurate and can provide predictive value for MACE, indicating CACS measures should be reported from these studies and factored into an individualized cardiovascular risk assessment.

Author Contributions

Conceptualization: GB JM ARM.

Data curation: GB AH BDY ES JM HJC WCW GC ARM.

Formal analysis: HJC WCW GC ES ARM.

Funding acquisition: ARM.

Investigation: GB AH BDY ES JM HJC WCW GC ARM.

Methodology: GB AH BDY ES JM HJC WCW GC ARM.

Project administration: ARM.

Resources: GB AH BDY JM HJC WCW GC ARM.

Software: GB AH BDY JM HJC WCW GC ARM.

Supervision: JM HJC WCW GC ARM.

Validation: GB AH BDY ES JM HJC WCW GC ARM.

Visualization: GB AH BDY ES JM HJC WCW GC ARM.

Writing – original draft: GB AH BDY JM HJC WCW GC ARM.

Writing – review & editing: GB AH BDY ES JM HJC WCW GC ARM.

References

1. WHO. The 10 leading causes of death in the world, 2000 and 2012: World Health Organization; 2012 [updated May 2014July 15, 2014]. http://www.who.int/mediacentre/factsheets/fs310/en/.

2. Budoff MJ, Mao S, Zalace CP, Bakhsheshi H, Oudiz RJ. Comparison of spiral and electron beam tomography in the evaluation of coronary calcification in asymptomatic persons. International journal of cardiology. 2001; 77(2–3):181–8. Epub 2001/02/22. PMID: 11182182

3. Rennenberg RJ, Kessels AG, Schurgers LJ, van Engelshoven JM, de Leeuw PW, Kroon AA. Vascular calcifications as a marker of increased cardiovascular risk: a meta-analysis. Vascular health and risk management. 2009; 5(1):185–97. Epub 2009/05/14. PMID: 19436645

4. Ehara S, Kobayashi Y, Yoshiyama M, Shimada K, Shimada Y, Fukuda D, et al. Spotty calcification typifies the culprit plaque in patients with acute myocardial infarction: an intravascular ultrasound study. Circulation. 2004; 110(22):3424–9. Epub 2004/11/24. https://doi.org/10.1161/01.CIR.0000148131.41425.E9 PMID: 15557374

5. Motoyama S, Sarai M, Harigaya H, Anno H, Inoue K, Hara T, et al. Computed tomographic angiography characteristics of atherosclerotic plaques subsequently resulting in acute coronary syndrome. Journal of the American College of Cardiology. 2009; 54(1):49–57. https://doi.org/10.1016/j.jacc.2009.02.068 PMID: 19555840

6. Puchner SB, Liu T, Mayrhofer T, Truong QA, Lee H, Fleg JL, et al. High-Risk Plaque Detected on Coronary CT Angiography Predicts Acute Coronary Syndromes Independent of Significant Stenosis in Acute Chest Pain: Results From the ROMICAT-II Trial. Journal of the American College of Cardiology. 2014; 64(7):684–92. https://doi.org/10.1016/j.jacc.2014.05.039 PMID: 25125300

7. Agatston AS, Janowitz WR, Hildner FJ, Zusmer NR, Viamonte M Jr., Detrano R. Quantification of coronary artery calcium using ultrafast computed tomography. Journal of the American College of Cardiology. 1990; 15(4):827–32. PMID: 2407762

8. Carr JJ, Nelson JC, Wong ND, McNitt-Gray M, Arad Y, Jacobs DR Jr., et al. Calcified coronary artery plaque measurement with cardiac CT in population-based studies: standardized protocol of Multi-Ethnic Study of Atherosclerosis (MESA) and Coronary Artery Risk Development in Young Adults (CARDIA) study. Radiology. 2005; 234(1):35–43. https://doi.org/10.1148/radiol.2341040439 PMID: 15618373

9. Sung JH, Yeboah J, Lee JE, Smith CL, Terry JG, Sims M, et al. Diagnostic Value of Coronary Artery Calcium Score for Cardiovascular Disease in African Americans: The Jackson Heart Study. Br J Med Med Res. 2016; 11(2). https://doi.org/10.9734/BJMMR/2016/21449 PMID: 26949662

10. Polonsky TS, McClelland RL, Jorgensen NW, Bild DE, Burke GL, Guerci AD, et al. Coronary artery calcium score and risk classification for coronary heart disease prediction. JAMA: the journal of the American Medical Association. 2010; 303(16):1610–6. https://doi.org/10.1001/jama.2010.461 PMID: 20424251

11. Collins FS, Varmus H. A new initiative on precision medicine. The New England journal of medicine. 2015; 372(9):793–5. https://doi.org/10.1056/NEJMp1500523 PMID: 25635347

12. Cancer Facts & Figures 2015. Atlanta: American Cancer Society, 2015 Contract No.: 09/20/2015.

13. Moyer VA, Force USPST. Screening for lung cancer: U.S. Preventive Services Task Force recommendation statement. Annals of internal medicine. 2014; 160(5):330–8. Epub 2014/01/01. https://doi.org/10.7326/M13-2771 PMID: 24378917

14. National Lung Screening Trial Research T, Aberle DR, Adams AM, Berg CD, Clapp JD, Clingan KL, et al. Baseline characteristics of participants in the randomized national lung screening trial. Journal of the National Cancer Institute. 2010; 102(23):1771–9. https://doi.org/10.1093/jnci/djq434 PMID: 21119104

15. Humphrey LL, Deffebach M, Pappas M, Baumann C, Artis K, Mitchell JP, et al. Screening for lung cancer with low-dose computed tomography: a systematic review to update the US Preventive services

task force recommendation. Annals of internal medicine. 2013; 159(6):411–20. https://doi.org/10.7326/0003-4819-159-6-201309170-00690 PMID: 23897166

16. National Lung Screening Trial Research T, Aberle DR, Adams AM, Berg CD, Black WC, Clapp JD, et al. Reduced lung-cancer mortality with low-dose computed tomographic screening. The New England journal of medicine. 2011; 365(5):395–409. https://doi.org/10.1056/NEJMoa1102873 PMID: 21714641

17. van den Bergh KA, Essink-Bot ML, Borsboom GJ, Th Scholten E, Prokop M, de Koning HJ, et al. Short-term health-related quality of life consequences in a lung cancer CT screening trial (NELSON). Br J Cancer. 2010; 102(1):27–34. https://doi.org/10.1038/sj.bjc.6605459 PMID: 19935789

18. Critchley JA, Capewell S. Mortality risk reduction associated with smoking cessation in patients with coronary heart disease: a systematic review. JAMA: the journal of the American Medical Association. 2003; 290(1):86–97. https://doi.org/10.1001/jama.290.1.86 PMID: 12837716

19. Jacobs PC, Gondrie MJ, van der Graaf Y, de Koning HJ, Isgum I, van Ginneken B, et al. Coronary artery calcium can predict all-cause mortality and cardiovascular events on low-dose CT screening for lung cancer. AJR American journal of roentgenology. 2012; 198(3):505–11. https://doi.org/10.2214/AJR.10.5577 PMID: 22357989

20. Mets OM, Vliegenthart R, Gondrie MJ, Viergever MA, Oudkerk M, de Koning HJ, et al. Lung cancer screening CT-based prediction of cardiovascular events. JACC Cardiovascular imaging. 2013; 6 (8):899–907. https://doi.org/10.1016/j.jcmg.2013.02.008 PMID: 23769488

21. Xie X, Zhao Y, de Bock GH, de Jong PA, Mali WP, Oudkerk M, et al. Validation and prognosis of coronary artery calcium scoring in nontriggered thoracic computed tomography: systematic review and meta-analysis. Circulation Cardiovascular imaging. 2013; 6(4):514–21. https://doi.org/10.1161/CIRCIMAGING.113.000092 PMID: 23756678

22. Bateman TM, Heller GV, McGhie AI, Friedman JD, Case JA, Bryngelson JR, et al. Diagnostic accuracy of rest/stress ECG-gated Rb-82 myocardial perfusion PET: comparison with ECG-gated Tc-99m sestamibi SPECT. J Nucl Cardiol. 2006; 13(1):24–33. https://doi.org/10.1016/j.nuclcard.2005.12.004 PMID: 16464714

23. Bengel FM, Higuchi T, Javadi MS, Lautamaki R. Cardiac positron emission tomography. Journal of the American College of Cardiology. 2009; 54(1):1–15. https://doi.org/10.1016/j.jacc.2009.02.065 PMID: 19555834

24. Buck AK, Nekolla S, Ziegler S, Beer A, Krause BJ, Herrmann K, et al. Spect/Ct. Journal of nuclear medicine: official publication, Society of Nuclear Medicine. 2008; 49(8):1305–19.

25. Di Carli MF. Hybrid imaging: integration of nuclear imaging and cardiac CT. Cardiol Clin. 2009; 27 (2):257–63, Table of Contents. https://doi.org/10.1016/j.ccl.2008.12.001 PMID: 19306768

26. Dorbala S, Di Carli MF, Delbeke D, Abbara S, DePuey EG, Dilsizian V, et al. SNMMI/ASNC/SCCT guideline for cardiac SPECT/CT and PET/CT 1.0. Journal of nuclear medicine: official publication, Society of Nuclear Medicine. 2013; 54(8):1485–507.

27. Einstein AJ, Johnson LL, Bokhari S, Son J, Thompson RC, Bateman TM, et al. Agreement of visual estimation of coronary artery calcium from low-dose CT attenuation correction scans in hybrid PET/CT and SPECT/CT with standard Agatston score. Journal of the American College of Cardiology. 2010; 56 (23):1914–21. https://doi.org/10.1016/j.jacc.2010.05.057 PMID: 21109114

28. Mylonas I, Kazmi M, Fuller L, deKemp RA, Yam Y, Chen L, et al. Measuring coronary artery calcification using positron emission tomography-computed tomography attenuation correction images. Eur Heart J Cardiovasc Imaging. 2012; 13(9):786–92. https://doi.org/10.1093/ehjci/jes079 PMID: 22511812

29. Kaster TS, Dwivedi G, Susser L, Renaud JM, Beanlands RS, Chow BJ, et al. Single low-dose CT scan optimized for rest-stress PET attenuation correction and quantification of coronary artery calcium. J Nucl Cardiol. 2015; 22(3):419–28. https://doi.org/10.1007/s12350-014-0026-y PMID: 25410469

30. Budoff MJ, Nasir K, Kinney GL, Hokanson JE, Barr RG, Steiner R, et al. Coronary artery and thoracic calcium on noncontrast thoracic CT scans: comparison of ungated and gated examinations in patients from the COPD Gene cohort. J Cardiovasc Comput Tomogr. 2011; 5(2):113–8. https://doi.org/10.1016/j.jcct.2010.11.002 PMID: 21167806

31. Hughes-Austin JM, Dominguez A 3rd, Allison MA, Wassel CL, Rifkin DE, Morgan CG, et al. Relationship of Coronary Calcium on Standard Chest CT Scans With Mortality. JACC Cardiovascular imaging. 2016; 9(2):152–9. https://doi.org/10.1016/j.jcmg.2015.06.030 PMID: 26777213

32. Kim SM, Chung MJ, Lee KS, Choe YH, Yi CA, Choe BK. Coronary calcium screening using low-dose lung cancer screening: effectiveness of MDCT with retrospective reconstruction. AJR American journal of roentgenology. 2008; 190(4):917–22. https://doi.org/10.2214/AJR.07.2979 PMID: 18356437

33. Takx RA, de Jong PA, Leiner T, Oudkerk M, de Koning HJ, Mol CP, et al. Automated coronary artery calcification scoring in non-gated chest CT: agreement and reliability. PloS one. 2014; 9(3):e91239. https://doi.org/10.1371/journal.pone.0091239 PMID: 24625525

34. Wu MT, Yang P, Huang YL, Chen JS, Chuo CC, Yeh C, et al. Coronary arterial calcification on low-dose ungated MDCT for lung cancer screening: concordance study with dedicated cardiac CT. AJR American journal of roentgenology. 2008; 190(4):923–8. https://doi.org/10.2214/AJR.07.2974 PMID: 18356438

35. Hanley JA, McNeil BJ. A method of comparing the areas under receiver operating characteristic curves derived from the same cases. Radiology. 1983; 148(3):839–43. https://doi.org/10.1148/radiology.148.3.6878708 PMID: 6878708

36. Hecht HS. Coronary artery calcium scanning: past, present, and future. JACC Cardiovascular imaging. 2015; 8(5):579–96. https://doi.org/10.1016/j.jcmg.2015.02.006 PMID: 25937196

37. Villines TC, Hulten EA, Shaw LJ, Goyal M, Dunning A, Achenbach S, et al. Prevalence and severity of coronary artery disease and adverse events among symptomatic patients with coronary artery calcification scores of zero undergoing coronary computed tomography angiography: results from the CONFIRM (Coronary CT Angiography Evaluation for Clinical Outcomes: An International Multicenter) registry. Journal of the American College of Cardiology. 2011; 58(24):2533–40. https://doi.org/10.1016/j.jacc.2011.10.851 PMID: 22079127

38. Chen J, Einstein AJ, Fazel R, Krumholz HM, Wang Y, Ross JS, et al. Cumulative exposure to ionizing radiation from diagnostic and therapeutic cardiac imaging procedures: a population-based analysis. Journal of the American College of Cardiology. 2010; 56(9):702–11. https://doi.org/10.1016/j.jacc.2010.05.014 PMID: 20619569

39. Gerber TC, Carr JJ, Arai AE, Dixon RL, Ferrari VA, Gomes AS, et al. Ionizing radiation in cardiac imaging: a science advisory from the American Heart Association Committee on Cardiac Imaging of the Council on Clinical Cardiology and Committee on Cardiovascular Imaging and Intervention of the Council on Cardiovascular Radiology and Intervention. Circulation. 2009; 119(7):1056–65. https://doi.org/10.1161/CIRCULATIONAHA.108.191650 PMID: 19188512

40. Berrington de Gonzalez A, Mahesh M, Kim KP, Bhargavan M, Lewis R, Mettler F, et al. Projected cancer risks from computed tomographic scans performed in the United States in 2007. Arch Intern Med. 2009; 169(22):2071–7. https://doi.org/10.1001/archinternmed.2009.440 PMID: 20008689

41. Sharma D, Newman TG, Aronow WS. Lung cancer screening: history, current perspectives, and future directions. Arch Med Sci. 2015; 11(5):1033–43. https://doi.org/10.5114/aoms.2015.54859 PMID: 26528348

42. Husmann L, Leschka S, Desbiolles L, Schepis T, Gaemperli O, Seifert B, et al. Coronary artery motion and cardiac phases: dependency on heart rate—implications for CT image reconstruction. Radiology. 2007; 245(2):567–76. https://doi.org/10.1148/radiol.2451061791 PMID: 17848683